The Adaptive Chirplet Transform and Visual Evoked Potentials

Article *in* IEEE transactions on bio-medical engineering · August 2006

DOI: 10.1109/TBME.2006.873700 · Source: PubMed

2 authors, including:

Richard J. Cui
Barrow Neurological Institute
31 PUBLICATIONS **692** CITATIONS

The Adaptive Chirplet Transform and Visual Evoked Potentials

Jie Cui, *Student Member, IEEE*, and Willy Wong* , *Member, IEEE*

***Abstract*—We propose a new approach based upon the adaptive chirplet transform (ACT) to characterize the time-dependent behavior of the visual evoked potential (VEP) from its initial transient portion (*t*VEP) to the steady-state portion (*ss*VEP). This approach employs a matching pursuit (MP) algorithm to estimate the chirplets and then a maximum-likelihood estimation (MLE) algorithm to refine the results. The ACT decomposes signals into Gaussian chirplet basis functions with four adjustable parameters, i.e., time-spread, chirp rate, time-center and frequency-center. In this paper, we show how these four parameters can be used to distinguish between the transient and the steady-state phase of the response. We also show that as few as three chirplets are required to represent a VEP response. Compared to decomposition with Gabor logons, a more compact representation can be achieved by using Gaussian chirplets. Finally, we argue that the adaptive chirplet spectrogram gives a superior visualization of VEP signals' time-frequency structures when compared to the conventional spectrogram.**

***Index Terms*—Chirplet transform, time-frequency analysis, *t*VEP and *ss*VEP, unified representation, visual evoked potentials.**

I. Introduction

VISUAL EVOKED potentials (VEPs) are surface electrical responses measured from the scalp in response to visual signals. It is believed that they are generated from the visual cortex and/or the peripheral neural pathways leading to the cortex and are time-locked to the visual stimulus [1]. VEPs have prominent clinical significance and can help diagnose sensory dysfunction [2]–[4]. More recently, VEPs have found applications in interface design, e.g., [5] and [6]. A variety of clinical applications (e.g., [5]–[8]) require the detection of steady-state visual evoked potentials (*ss*VEPs) which are elicited by stimuli of sufficiently high repetition frequency. Under steady-state conditions a VEP signal can be modeled in terms of a fundamental sinusoid and higher harmonics. The model however is incomplete as it is believed that a transient component (*t*VEP) appears first following the onset of the visual stimulus [2], [9]. Moreover, given the variability in a subject's mental state, a true steady-state response is hard to achieve under normal recording conditions. Therefore, a linear expansion from a Fourier basis may not be the optimal way to represent the signal.

It should be emphasized that the term "transient VEP," or *t*VEP, employed here is conceptually different from that used in traditional electrophysiological literature. It usually refers to an experimental paradigm where the potentials are evoked by visual stimuli which are sufficiently widely spaced so that the visual system can be regarded as returning to a state of rest between successive stimuli [2]. In this paper, however, *t*VEP refers to the preceding signal process before the formation of steady-state VEP. Usually, it is different from EP evoked with low stimulus rates.

Recently, a number of applications require fast estimation and detection of VEPs (e.g., [6]). This has prompted us to find new ways to characterize the transient portion of the response. Our approach provides a unified representation of the *complete* VEP response (both transient and steady-state VEPs). We have not seen this in competing techniques. A unified approach can benefit many types of physiological and electrophysiological studies including those investigating the time course of visual cortical activity [10]–[13].

In this paper, we present a new technique based upon the chirplet transform (CT) [14], which allows us to clearly visualize, perhaps for the first time, the early moments of a VEP response. We have implemented this technique by adopting the adaptive algorithm of the matching pursuit (MP) with chirplets [15]. Our approach also incorporates a maximum-likelihood estimation (MLE) algorithm to help estimate the signal under the low signal-to-noise ratio (SNR) conditions that are typical of VEP measurements. It has been shown that the MP algorithm with Gabor logons (i.e., time-frequency atoms of windowed sinusoids) can yield good performance [16]–[18]. But our approach enables us to achieve a more compact representation of VEPs over the complete response. Finally, we demonstrate that the adaptive chirplet spectrogram (ACS) yields a better visualization of VEP decompositions compared to the traditional, short-time Fourier transform (STFT) based spectrogram [19].

The adaptive chirplet transform (ACT) can also be applied to the analysis of other types of biomedical signals such as raw electroencephalogram (EEG) of sufficiently high SNR. For time-locked EEG phenomena with low SNR (such as the VEP discussed in this paper), one may need to obtain an ensemble average of the signals before applying the ACT.

In the next section, we introduce the adaptive chirplet decomposition and show the implementation of our algorithm. In Section III, the experimental method is described. The results and discussions are found in Section IV and finally the major findings are summarized in Section V.

II. Computational Approach

A. The Adaptive Chirplet Decomposition

The CT has been under continual development over the past ten years [14], [15], [17], [20]–[24]. A "chirp" or chirp function

Manuscript received September 12, 2005; revised January 16, 2006. This work was supported by NSERC Canada.

J. Cui is with the Institute of Biomaterials and Biomedical Engineering, University of Toronto, Toronto, ON M5S 3G9, Canada.

*W. Wong is with the Department of Electrical and Computer Engineering and the Institute of Biomaterials and Biomedical Engineering, University of Toronto, 164 College Street, Toronto, ON M5S 3G4, Canada (e-mail: willy@eecg.utoronto.ca). *Asterisk indictaes corresponding author.*

Digital Object Identifier 10.1109/TBME.2006.873700

is a rapidly swept sinusoidal wave and a "chirplet" is a windowed chirp function. The STFT (or windowed Fourier transform) and wavelet transform (WT) may be loosely considered as special cases of the CT [14]. The main deficiency of STFT is that the length of the window is fixed and, thus, is not an effective way to describe structures much smaller or much larger than the window length. Although the wavelet transform overcomes this limitation by allowing for a variable window length, there is a fundamental reciprocal relation that exists between the central frequency of a wavelet and its window length. Therefore, the wavelet transform does not provide precise estimates of low frequency components with short-time duration or narrow-band high frequency components. In the wavelet transform, the basis functions are derived from a single mother wavelet by two operations of dilation and translation [25]. Similarly, the bases for a Gaussian CT are derived from a single Gaussian function $\pi^{-1/4}\exp(-t^2/2)$ through four operations: scaling, chirping, time- and frequency-shifting, which leads to a family of wave packets with four adjustable parameters [14]

$$g_{t_c,\omega_c,c,\Delta_t}(t) = \frac{1}{\sqrt{\sqrt{\pi}\Delta_t}} e^{-\frac{1}{2}\left(\frac{t-t_c}{\Delta_t}\right)^2} e^{j[c(t-t_c)+\omega_c](t-t_c)} \quad (1)$$

where $j=\sqrt{-1}$, t_c is the time center, ω_c the frequency center, $\Delta_t > 0$ the effective time-spread, and c the chirp rate that characterizes the "quickness" of frequency changes. Subsequently, the transform of a signal is defined as the inner product between the signal $f(t)$ and the Gaussian chirplet $g_{t_c,\omega_c,c,\Delta_t}$ defined in (1)

$$a_{t_c,\omega_c,c,\Delta_t} = \int_{\infty}^{-\infty} f(t) g^*_{t_c,\omega_c,c,\Delta_t}(t)dt \quad (2)$$

where "$*$" denotes the complex conjugate operation. The coefficient $a_{t_c,\omega_c,c,\Delta_t}$ represents the signal's energy content in a time-frequency region specified by the chirplets, and the absolute value of the coefficient is the amplitude of the projection. To simplify the notation, the set of chirplet parameters is described by a continuous index set $I=(t_c,\omega_c,c,\Delta_t)$. An arbitrary signal $f(t)$ is then constructed as a linear combination of Gaussian chirplets, i.e.,

$$\begin{aligned} f(t) &= \sum_{n=1}^{P} a_{I_n} g_{I_n}(t) + R^{P+1} f(t) \\ &= f_P(t) + R^{P+1} f(t) \end{aligned} \quad (3)$$

where I_n is the parameter set of the nth chirplet, $R^{P+1}f(t)$ denotes the residue and $f_P(t)$ is defined as the Pth-order approximation of the signal. Since $g_{I_n}(t)$ has a Gaussian envelope, minimum time-frequency variance is achieved [26]. Note that the coefficient a_{I_n} is complex and hence the decomposition information at each iteration n is described by six real parameters, i.e., two from a_{I_n} and the other four from I_n.

The optimal estimation of a_{I_n} and I_n corresponding to the decomposition of a signal into the basis functions g_{I_n} is an NP-hard problem [27]. This means that no known polynomial time algorithm exists to solve this operation. Consequently, there have been efforts to develop suboptimal techniques

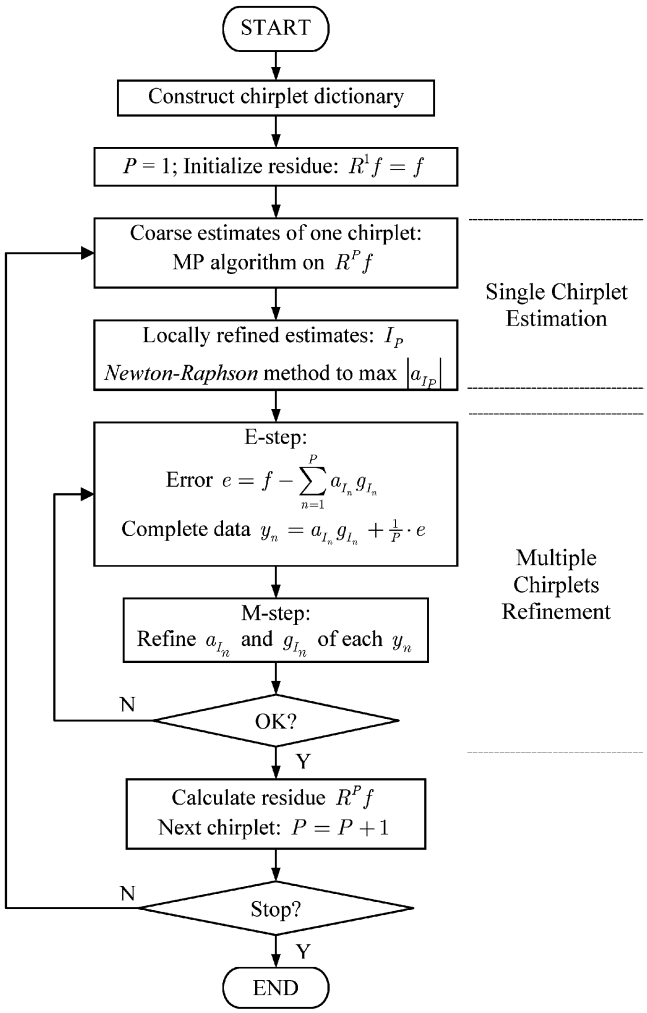

Fig. 1. Flowchart of the adaptive chirplet decomposition algorithm.

[15]–[17], [28] and we will describe one such approach next. The essence of this approach is to approximate the signal's energy curve on the time-frequency plane using straight lines with arbitrary slopes [24]. To decompose a given signal into multiple chirplets two crucial procedures are involved at each iterative step of our approach: 1) initial coarse estimates of chirplets are obtained using the MP algorithm; 2) the estimates undergo progressive refinement with the MLE algorithm. The implementation of this adaptive chirplet decomposition algorithm is illustrated by the flowchart in Fig. 1. The initialization stage of the algorithm consists of the construction of a chirplet "dictionary" and the initial residue: $R^1 f = f$ (i.e., the original signal itself). The dictionary is constructed according to [15], namely a set of finite predetermined chirplets selected to cover the entire time-frequency plane. In the estimation of a single chirplet, the task is to find the parameters that maximize the amplitude of the projection defined in (2) as implemented using the MP algorithm. In essence, the amplitudes are obtained from projecting the residue $R^P f(t)$ onto each chirplet in the dictionary and the optimal chirplet is decided on the basis of the projection amplitude. From these results (termed "coarse estimation"), we further optimize the values using a *Newton–Raphson* method to refine the match locally. After

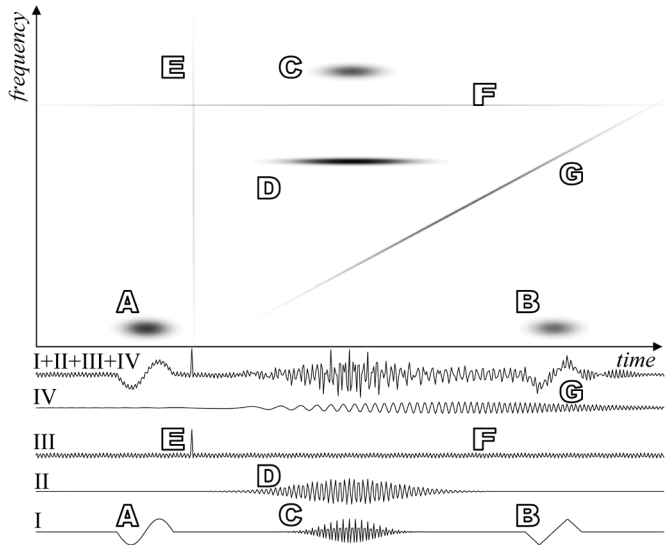

Fig. 2. ACS of the simulated signal. The simulated signal is a sum of signal structures I–IV, which is shown directly below the ACS. The horizontal axis is time in seconds and the vertical axis is frequency in Hz.

the single chirplet $g_{I_n}(t)$ and its coefficient a_{I_n} have been decided from $R^P f(t)$, it is subtracted from the signal and a new chirplet is then estimated from the residue $R^{P+1}f(t)$. We emphasize that the adaptive nature of the mechanism of the algorithm comes from the optimal selection of the basis functions (i.e., chirplets) for decomposition. The parameters of these functions are predefined in the dictionary, which differs from the approach of adaptive filtering where the parameters are varied on a sample by sample basis [29].

In the case of estimating multiple chirplets, we employ an iterative procedure similar to the proposed methods [16], [30]. Note however that these methods generally assume a signal model without noise and hence their efficiency under very low SNR conditions has not been rigorously demonstrated. This is of relevance to our problem since VEP signals are often obtained under low SNR conditions. Recently, an alternative algorithm based upon the principle of MLE has been proposed [22]. Following this idea, we have adopted the expectation-maximization (EM) algorithm to further refine the estimates of the chirplets. More specifically, the EM algorithm consists of two steps: an expectation step (E step) and a maximization step (M step). In the E step the complete data y_n for $n = 1, \ldots, P$ are calculated as follows:

$$e = f - \sum_{n=1}^{P} a_{I_n} g_{I_n} \tag{4}$$

$$y_n = a_{I_n} g_{I_n} + \frac{1}{P} e, \quad n = 1, \ldots, P. \tag{5}$$

The M step applies the same algorithm employed in the estimation of a single chirplet to each of the y_n to refine the estimate of this chirplet. The EM algorithm may be repeated several times until the error in (4) is below a predefined level.

The simulation shown in Fig. 2 illustrates the performance of our technique. In this analysis, we show the decomposition of a complex signal into a number of Gaussian chirplets based upon our algorithm. The ACS—which is a direct sum of the Wigner-Ville distributions of the individual chirplets—clearly shows the time-frequency structures of the signal. Note that the waveforms A–F are similar to those in the simulation found in [18] where the MP algorithm with Gabor logons was used. However, the chirping structure "G" cannot be represented efficiently using Gabor logons.

B. Measures for Stopping Criterion and Compactness

A critical point of the analysis is the determination of the number of chirplets required to sufficiently represent the VEP signals. We did not attempt to predefine this number, but rather to continue the decomposition until a specific stopping criterion is satisfied. One method of approach is to calculate the coherent coefficients (CC) of the extracted chirplets, which is defined as a ratio of the energy of the projection to the residue

$$cc_n = \frac{|a_{I_n}|^2}{\|R^n f\|^2}, \quad n = 1, \ldots, P \tag{6}$$

where $|a_{I_n}|$ is the energy of the projection, the absolute square of the coefficient of the nth chirplet, and $\|R^n f\|^2$ is the energy of the residue, i.e., $R^n f = f - \sum_{i=1}^{n-1} a_{I_i} g_{I_i}$. This measure was originally proposed in [16] to characterize the coherence of a signal with respect to the dictionary of functions. In other words, the chirplets in the dictionary serve as a "vocabulary to interpret a given sentence." The more coherent a signal with respect to the dictionary, the larger the CC values. Therefore, a small CC value indicates the low correlation between the signal and the dictionary. A threshold based upon the CC value can be chosen for a stopping criterion. In Section IV, we give out the criterion using CC values according to the estimated chirplets.

Another measure is derived from the energy ratio (ER) which is the ER of the residue to the original signal

$$\mathrm{ER}_n = \frac{\|R^n f\|^2}{\|f\|^2}. \tag{7}$$

Later, we will employ this measure to compare the compactness of the chirplet representation with that of the Gabor logon representation in Section IV.

III. Data Acquisition Method

The visual stimulus was a matrix of moving bars denoted by MMB, which follows essentially the pattern adopted in [31] (see Fig. 3). With a central cross this display consists of a series of 16 horizontal/vertical bar pairs, 1.2° high and 0.2° wide each bar, distributed evenly across a display subtending over a 10.5° visual angle and with a contrast equal to 40%. All stimuli were produced on a liquid-crystal display monitor (ViewSonic ViewPanel VP150m) using a high-resolution graphics board (Nvidia GeForce4, 1024 by 768 pixels, 75 Hz). The display had an approximate mean luminance of 50 $\mathrm{cd/m^2}$.

Five healthy adult subjects participated in this study. They all had normal or corrected to normal vision with no known impairment to their visual systems. The subjects viewed the monitor binocularly from a distance of 50 cm in a darkened room. VEPs were recorded via gold-cup electrodes applied to the scalp

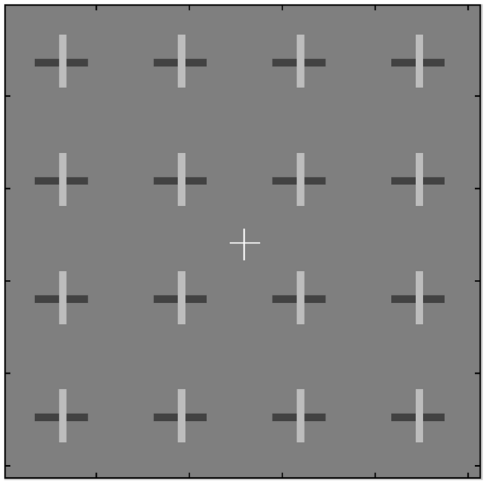

Fig. 3. Matrix of moving bars (MMB).

with TEN20 electrolyte paste following skin preparation using NU-PREP abrasive gel. The active electrodes were placed on the scalp at Oz of the International 10–20 System, while the electrode on the right ear lobe served as the reference. The third electrode, placed on the left ear lobe, acted as ground. The contact impedance of the three electrodes was below 10 kΩ for all subjects. The EEG signal was amplified (by a Grass CP511 AC amplifier at 1000 folds), bandpass-filtered (0.01 Hz–300 Hz), passed through an analog-to-digital converter (NI PCI-4451, 16-bit, sampled at 1 kHz) and then streamed to the harddisk. At the start of post-recording analysis (carried off-line), the data was further lowpass-filtered at 40 Hz (-3 dB) with a FIR digital filter and then re-sampled at 240 Hz.

A single trial consisted of 5 s of data. Following a 1-s prestimulation period, the vertical bars began oscillating in the horizontal direction with temporal frequency of 3.0 ± 0.1 Hz for 4 s, while the 16 horizontal bars remained static and served as the positional reference for the vertical bars. The onset of the stimuli was at the end of the first second. The relative amplitude of the motion was 40% of the horizontal bar length. The subjects were instructed to pay attention to the moving bars on the screen. Eye movements were minimized by having the subjects fix their gaze at the central cross. They were also asked to withhold eye blinks during each trial and to keep their facial muscles relaxed. Each subject sat for a total of 50 trials. S/he initiated the trials with a button when s/he was ready. The subjects were previously trained before the start of the session to ensure that they understood the task.

IV. Results and Discussion

An averaged signal was obtained from the 50 trails of a single subject. In total, we obtained five averaged signals (denoted D_1–D_5) from the five subjects. The algorithm was implemented by using Matlab 7.0 on a Pentium IV PC (3.0 GHz) with 1.0 GB memory. The average time taken to estimate one chirplet from a 1200-point signal was approximately 8 min. For each of the averaged signals, ten Gaussian chirplets were estimated with the algorithm described in Fig. 1. We believe this number of chirplets is sufficient for representing the VEP of interest as the residue after ten iterations was close to white noise (Fig. 8, discussed below). As an example, Table I summarizes the estimated parameters of the ten chirplets extracted from D_1 along with the coherent coefficients cc_n. In general, the chirplets extracted first had higher amplitudes and higher CC values. Particularly, we found that the amplitudes of the first three chirplets are significantly higher than those of the remaining chirplets. The first chirplet, c_1, represents the steady-state component of the VEP signal as it has a long time-spread, $\widehat{\Delta}_t$, and a near zero chirp rate. The remaining two chirplets c_2 and c_3 have negative chirp rates, indicating that the instantaneous frequency decreased with time.

TABLE I
Ten Chirplets Estimated From Signal D_1 and Their Coherent Coefficients

Chirplets†	$\widehat{a}$	$\widehat{\phi}$(rad)	$\widehat{t}_c$(s)	$\widehat{f}_c$(Hz)	$\widehat{c}$(Hz/s)	$\widehat{\Delta}_t$(s)	cc_n
c_1	198.97	-2.18	3.56	5.59	-0.01	1.02	0.17
c_2	174.84	2.50	1.82	6.00	-1.35	0.26	0.17
c_3	131.53	1.40	1.47	7.75	-50.07	0.05	0.11
c_4	94.40	1.10	2.02	15.16	17.79	0.41	0.07
c_5	88.66	0.32	1.25	18.26	1.10	0.69	0.06
c_6	74.14	-2.23	4.80	8.38	-8.30	0.20	0.05
c_7	86.68	1.25	3.89	11.30	0.12	0.76	0.07
c_8	75.19	0.18	1.70	26.33	-0.42	1.01	0.05
c_9	66.76	-0.78	0.24	10.88	3.04	0.16	0.05
c_{10}	67.07	-2.77	1.02	34.37	2.05	0.78	0.05

†The 10 chirplets are labeled as $c_1 - c_{10}$. The estimated parameters are in reference to equation (1). 'cc_n' is the coherent coefficient.

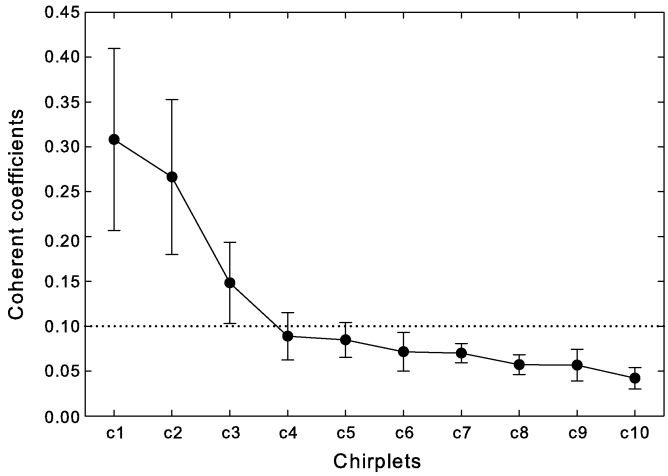

Fig. 4. Statistic of the coherent coefficients.

To facilitate the determination of the stopping criterion, the mean and standard deviation (SD) of CC values of the ten chirplets from all five signals are summarized in Fig. 4. It can be seen that the values decrease with each increasing step.[1] Typically, the CC values of the first three chirplets are significantly higher than 0.10, indicating that the first three or four chirplets are usually sufficient to represent VEP signals assuming a cutoff at 0.10 (cf. Figs. 5 and 6). This provides a reasonable stopping criterion for our data.

Fig. 5 shows the visualization of the results in Table I using the adaptive chirplet spectrogram (ACS) and compares it to the conventional spectrogram calculated by STFT. Below the spectrogram in [Fig. 5(A)] is the signal D_1 with the spectrum shown

[1]Since only one chirplet is estimated in each iterative step, the indices of the steps are identical to the indices of the chirplets.

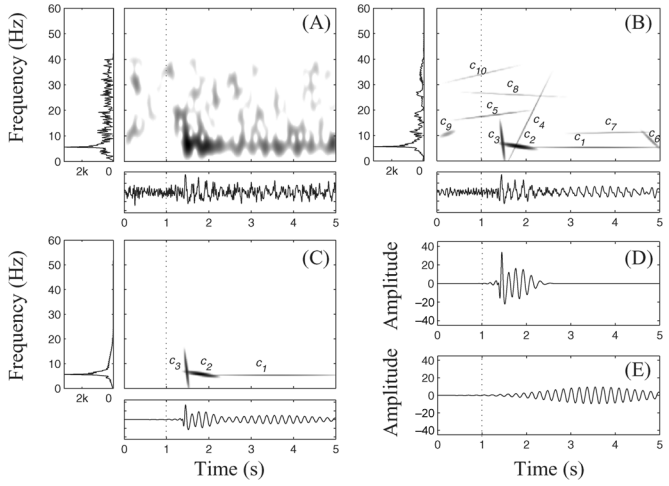

Fig. 5. Example: time-frequency analysis of signal D_1. (A) Spectrogram of D_1 (with 11-point Gaussian window); immediately below is the waveform of D_1; the signal's spectrum is shown on the left. (B) ACS of the ten chirplets with the reconstructed signal (below) and its spectrum (left). (C) Chirplets c_1–c_3 as VEP representation. (D) Reconstructed signal (from c_2 and c_3) representing *t*VEP. (E) Reconstructed signal (from c_1) representing *ss*VEP.

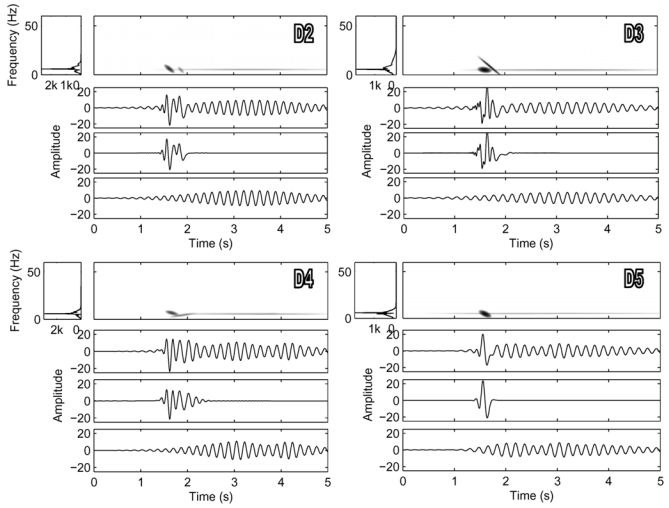

Fig. 6. ACSs of chirplets with CC values above 0.10 from signals D_2–D_5 (averaged signals from subjects 2–5). Spectrum of the reconstructed signal is shown on the left. The reconstructed signal, the *t*VEP and *ss*VEP components are shown immediately below the spectrogram.

on the left. The vertical dotted lines at 1 s represent the onset of visual stimuli. Fig. 5(B) shows the ACS of the ten chirplets accompanied by the reconstructed signal shown directly below and the spectrum on the left. It can be seen that the reconstructed signal provides a "less noisy" waveform. Chirplets c_1–c_3 are shown separately in Fig. 5(C). These three chirplets $(cc_{1-3} > 0.10)$ show a typical representation of VEPs. In Fig. 5(D) and (E), as discussed later, we partitioned the signal into its transient and steady-state components by reconstructing the steady-state portion using c_1 and the transient using c_2 and c_3.

The experimental results of other subjects are reported in Fig. 6. The ACS shows the chirplets with CC values above 0.10. It can be seen that the results generally mirror the results shown for signal D_1. The statistic of the extracted parameters are summarized in Table II. It can be seen that the values of the time-spread and the time-center are significantly different for the transient and steady-state components. *ss*VEPs have much

TABLE II
STATISTIC OF THE PARAMETERS OF TRANSIENT AND STEADY-STATE VEPS

	*t*VEP	*ss*VEP
$\widehat{c}$ (Hz/s)	-13.45 $\pm$ 15.98	-0.01 $\pm$ 0.02
$\widehat{\Delta}_t$ (s)	0.12 $\pm$ 0.08	1.14 $\pm$ 0.14
$\widehat{t}_c$ (s)	1.69 $\pm$ 0.14	3.31 $\pm$ 0.20
$\widehat{f}_c$ (Hz)	6.34 $\pm$ 1.35	5.74 $\pm$ 0.16

TABLE III
ERS CALCULATED FROM THE DECOMPOSITION USING CHIRPLETS, $\mathrm{ER_C}$

sig.†	$n=1$	2	3	4	5	6	7	8	9	10
D_1	0.78	0.63	0.55	0.53	0.49	0.48	0.44	0.42	0.40	0.38
D_2	0.55	0.41	0.36	0.34	0.32	0.30	0.28	0.27	0.25	0.24
D_3	0.78	0.63	0.58	0.50	0.44	0.41	0.38	0.35	0.33	0.32
D_4	0.50	0.37	0.28	0.25	0.23	0.21	0.19	0.18	0.17	0.16
D_5	0.84	0.50	0.46	0.44	0.39	0.35	0.33	0.31	0.28	0.26
Mean	0.69	0.51	0.45	0.41	0.37	0.35	0.32	0.30	0.29	0.27
STD	0.15	0.12	0.12	0.11	0.10	0.10	0.09	0.09	0.09	0.08

†$D_1 - D_5$ are the measured signals from the five subjects.

TABLE IV
ERS CALCULATED FROM THE DECOMPOSITION USING GABOR LOGONS, $\mathrm{ER_G}$

sig.	$n=1$	2	3	4	5	6	7	8	9	10
D_1	0.76	0.67	0.63	0.60	0.58	0.56	0.55	0.54	0.52	0.51
D_2	0.57	0.49	0.47	0.46	0.45	0.45	0.43	0.43	0.43	0.42
D_3	0.79	0.71	0.62	0.58	0.55	0.53	0.50	0.49	0.47	0.46
D_4	0.50	0.43	0.40	0.38	0.35	0.34	0.33	0.33	0.32	0.28
D_5	0.77	0.76	0.73	0.71	0.70	0.68	0.66	0.65	0.63	0.62
Mean	0.68	0.61	0.57	0.54	0.52	0.51	0.50	0.49	0.47	0.46
STD	0.13	0.15	0.13	0.13	0.13	0.13	0.13	0.12	0.11	0.12

wider time-spread (typically, $\widehat{\Delta}_t \geq 1$) and a later time of appearance (typically, $\widehat{t}_c \geq 3.21$). Moreover both the chirp rate and the variance are close to zero at steady-state. Thus, we adopted the following criteria to classify the different components: a chirplet describes the steady-state if: 1) its time-spread is wider than 1 s; 2) its time-center is later than 2.21 s after the stimulus onset; 3) the chirp rate is less than 0.03 Hz/s. The remaining chirplets are then classified as transients.

In general, we concluded from our data that a 1200-point, 5 s, VEP response can be well represented by as few as three chirplets (see, however, later discussion on the whiteness of residue). This represents a total of 18 parameters (4 parameters per chirplet plus amplitude and phase). We can, thus, achieve a very sparse representation of the original VEP signal. Furthermore, the conventional information of EP analysis such as amplitude and latency of the signal has been retained and can be retrieved easily from the reconstructed signal.

Earlier in the article, we had claimed that a main feature to our approach is that the VEP response can be more compactly represented using chirplets. We evaluated the compactness of our approach by comparing the number of atoms[2] required to reconstruct a signal using either chirplets or Gabor logons. The only difference between the two techniques lies in the composition of the dictionary. We compared the compactness of the decomposition by using the measure of ER defined in (7). The values calculated from the chirplet decompositions (ER_C) and the Gabor logons decompositions (ER_G) are shown in Tables III and IV

[2]We here loosely use the term "atom" to refer to the basis function involved in decomposition, i.e., either a chirplet or a Gabor logon.

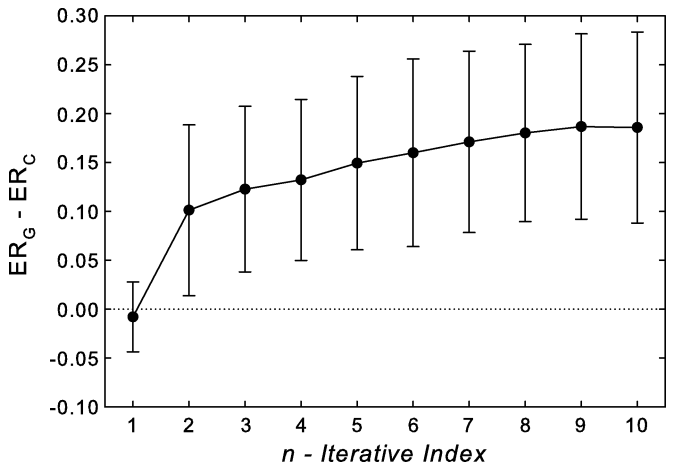

Fig. 7. Mean and SD values of the energy-ratio differences.

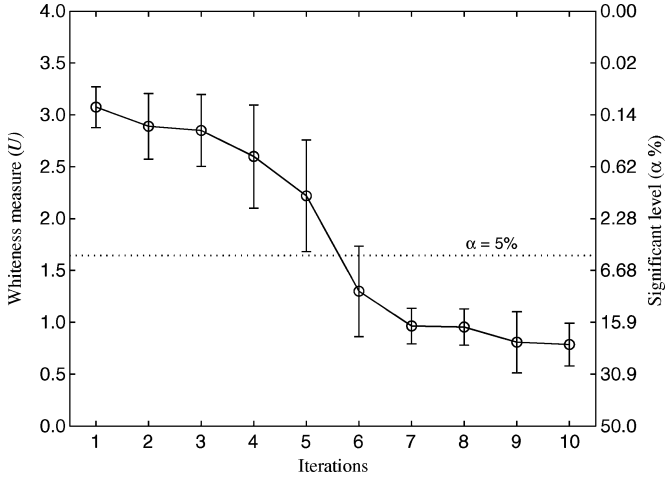

Fig. 8. Mean and SD values of the whiteness measure of signal residues. For each of the five signals D_1–D_5 (averaged signals from subjects 2–5), the whiteness measures (U) of signal residues after each of the iterations were calculated and the mean and SD values were obtained across the subjects.

respectively. The difference in energy extraction between the two techniques was evaluated by calculating $\mathrm{ER}_G - ER_C$ and the statistic. Fig. 7 clearly shows that except for the very first step, the decomposition with chirplet extracts more energy than the decomposition with Gabor logons at each iterative step. To see why the first step shows no statistical difference, we recall that the first atom extracted is the one that represents the steady-state portion of VEP signals. Thus, we expect both methods to yield the same result.

The ACS approach described in this paper allows us to visualize the time-frequency structure of the VEP response at higher resolution than previously possible. Spectrograms that have been constructed using STFT will invariably involve smoothing of some sort yielding an overall lower resolution picture [26]. Although the spectrogram can show some of the salient time-frequency structures of the VEP response, most of the detail is lost due to smearing. However, as we have shown with the ACS, e.g., Fig. 5(B) and (C), the resulting time-frequency decomposition provides a clear picture of the underlying process. The estimated parameters obtained from the decomposition analysis provide detailed information about the local time-frequency structures of the signal not easily obtainable from the standard spectrogram alone.

By adopting the MLE algorithm, our approach assumes a signal model that the VEP signal can be represented by a weighted sum of chirplets in additive Gaussian white noise. To verify our model, we employed a statistic measure of whiteness (U), proposed by Drouiche [32], to test the whiteness of the residual signals after each iterative steps. Specifically, we test against the null hypothesis (H_0) that the residue is white. If U is larger than the critical value calculated according to a predefined threshold of significant level α [32], then the residue is not white (H_1). Typically, α is set at 5% and $t_{0.05} = 1.65$. The mean and SD values of the whiteness measures are shown in Fig. 8. The measures were calculated after each of the iterations and then averaged across subjects. Given a 5% significant level, we see that the residue is white after approximately six iterations. That is, the VEP can be completely represented by six chirplets. However, the first three estimated chirplets with the CC values above 0.10 (Fig. 4) may be regarded as the major components with respect to a given dictionary, since they appear to characterize the major time-frequency variation of a VEP signal.

From Figs. 5 and 6, it appears that Gaussian chirplets cannot properly represent the steady-state portion of the VEP response, since the reconstructed signal suggests that the steady-state VEP decreases in amplitude after 4 s, which is not evident in the measured signals (e.g., signal D_1 in Fig. 5). This artifact is in fact a limitation caused by the Gaussian envelope of the chirplet as the bell-shaped envelope diminishes in amplitude at both ends. There are a number of ways to resolve this shortcoming including increasing the number of chirplets used to construct the steady-state portion of the signal or by including Fourier components (long-duration sinusoids) in the dictionary vocabulary as suggested in [16].

Finally, the local time-frequency structures that cannot be efficiently matched by a single chirplet will be represented by several chirplets. Should the structures prove to be important, it is easy enough to expand the vocabulary by including these structures directly within the dictionary. An automatic procedure to expand the dictionary for new biomedical signals is an interesting future research question.

V. Conclusion

The ACT technique provides information on the local time-frequency structures of both prestimulation and post-stimulation of VEP signals at higher resolution than previously possible. The estimated parameters can help distinguish different components of the VEP response. Only a small number of components are required to represent the entire VEP response. The adaptive spectrogram also yields an improved visualization of the time-frequency information contained in the signal. Our technique of VEP estimation can serve as an alternative to conventional spectral analysis and band-pass filtering technique.

ACKNOWLEDGMENT

The authors thank Dr. M. R. Popovic, Dr. H. Kunov, and Dr. S. Mann of University of Toronto for their valuable comments related to this work.

REFERENCES

[1] D. Regan, *Evoked Potentials in Psychology, Sensory Physiology and Clinical Medicine*. London, U.K.: Chapman & Hall, 1972.
[2] ——, *Human Brain Electrophysiology: Evoked Potentials and Evoked Magnetic Fields in Science and Medicine*. New York: Elsevier, 1989.
[3] A. M. Halliday, *Evoked Potentials in Clinical Testing*, 2nd ed. U.K.: Churchill Livingstone, 1992.
[4] J. R. Heckenlively and G. B. Arden, *Principles and Practice of Clinical Electrophysiology of Vision*. St Louis, MO: Mosby Year Book, 1991.
[5] M. Middendorf, G. McMillan, G. Calhoun, and K. S. Jones, "Brain-computer interfaces based on the steady-state visual-evoked response," *IEEE Trans. Rehabil. Eng.*, vol. 8, no. 2, pp. 211–214, Jun. 2000.
[6] M. Cheng, X. R. Gao, S. G. Gao, and D. F. Xu, "Design and implementation of a brain-computer interface with high transfer rates," *IEEE Trans. Biomed. Eng.*, vol. 49, no. 10, pp. 1181–1186, Oct. 2002.
[7] C. E. Davila and R. Srebro, "Subspace averaging of steady-state visual evoked potentials," *IEEE Trans. Biomed. Eng.*, vol. 47, no. 6, pp. 720–728, Jun. 2000.
[8] A. P. Liavas, G. V. Moustakides, G. Henning, E. Z. Psarakis, and P. Husar, "A periodogram-based method for the detection of steady-state visually evoked potentials," *IEEE Trans. Biomed. Eng.*, vol. 45, no. 2, pp. 242–248, Feb. 1998.
[9] L. H. Van Der Tweel, "Relation between psychophysics and electrophysiology of flicker," *Documenta Ophthalmologica*, vol. 18, pp. 287–304, 1964.
[10] W. A. Ho and M. A. Berkley, "Evoked-potential estimates of the time course of adaptation and recovery to counterphase gratings," *Vision Res.*, vol. 28, pp. 1287–1296, 1988.
[11] N. S. Peachey, P. J. Demarco, R. Ubilluz, and W. Yee, "Short-term changes in the response characteristics of the human visual-evoked potential," *Vision Res.*, vol. 34, pp. 2823–2831, 1994.
[12] D. Y. Xin, W. Seiple, K. Holopigian, and M. J. Kupersmith, "Visual-evoked potentials following abrupt contrast changes," *Vision Res.*, vol. 34, pp. 2813–2821, 1994.
[13] C. Janz, S. P. Heinrich, J. Kornmayer, M. Bach, and J. Hennig, "Coupling of neural activity and BOLD fMRI response: new insights by combination of fMRI and VEP experiments in transition from single events to continuous stimulation," *Magn. Reson. Med.*, vol. 46, pp. 482–486, 2001.
[14] S. Mann and S. Haykin, "The chirplet transform—physical considerations," *IEEE Trans. Signal Process.*, vol. 43, no. 11, pp. 2745–2761, Nov. 1995.
[15] A. Bultan, "A four-parameter atomic decomposition of chirplets," *IEEE Trans. Signal Process.*, vol. 47, no. 3, pp. 731–745, Mar. 1999.
[16] S. G. Mallat and Z. Zhang, "Matching pursuit with time-frequency dictionaries," *IEEE Trans. Signal Process.*, vol. 41, no. 12, pp. 3397–3415, Dec. 1993.
[17] R. Gribonval, "Fast matching pursuit with a multiscale dictionary of Gaussian chirps," *IEEE Trans. Signal Process.*, vol. 49, no. 5, pp. 994–1001, May 2001.
[18] P. J. Durka and K. J. Blinowska, "Analysis of EEG transients by means of matching pursuit," *Ann. Biomed. Eng.*, vol. 23, pp. 608–611, Sept. 1995.
[19] M. Akay, *Time-Frequency and Wavelets in Biomedical Signal Processing*. New York: IEEE Press, 1998.
[20] S. Mann and S. Haykin, "Adaptive chirplet transform—an adaptive generalization of the wavelet transform," *Opt. Eng.*, vol. 31, pp. 1243–1256, Jun. 1992.
[21] D. Mihovilovic and R. N. Bracewell, "Adaptive chirplet representation of signals on time frequency plane," *Electron. Lett.*, vol. 27, pp. 1159–1161, Jun. 1991.
[22] J. C. O'Neill and P. Flandrin, "Chirp hunting," in *Proceedings of the IEEE-SP International Symposium on Time-Frequency and Time-Scale Analysis*, 1998, pp. 425–428.
[23] R. G. Baraniuk and D. L. Jones, "Wigner-based formulation of the chirplet transform," *IEEE Trans. Signal Process.*, vol. 44, no. 12, pp. 3129–3135, Dec. 1996.
[24] H. X. Zou, Y. Q. Chen, J. H. Zhu, Q. H. Dai, G. Q. Wu, and Y. D. Li, "Steady-motion-based Dopplerlet transform: application to the estimation of range and speed of a moving sound source," *IEEE J. Ocean. Eng.*, vol. 29, no. 3, pp. 887–905, Jul. 2004.
[25] I. Daubechies, *Ten Lectures on Wavelets*. Philadelphia, PA: Soc. Ind. Appl. Math. (SPIE), 1992.
[26] L. Cohen, *Time-Frequency Analysis*. Upper Saddle River, N.J: Prentice-Hall PTR, 1995.
[27] G. Davis, S. Mallat, and M. Avellaneda, "Adaptive greedy approximations," *Constructive Approximation*, vol. 13, pp. 57–98, 1997.
[28] S. Qian, D. P. Chen, and Q. Y. Yin, "Adaptive chirplet based signal approximation," in *Proc. 1998 IEEE Int. Conf. Acoustics, Speech, and Signal Processing*, 1998, vol. 1–6, pp. 1781–1784.
[29] S. J. Orfanidis, *Optimum Signal Processing: An Introduction*, 2nd ed. New York: Macmillan, 1988.
[30] S. Qian and D. P. Chen, "Signal representation using adaptive normalized Gaussian functions," *Signal Process.*, vol. 36, pp. 1–11, 1994.
[31] F. Pei, M. W. Pettet, and A. M. Norcia, "Neural correlates of object-based attention," *J. Vision*, vol. 2, pp. 588–596, 2002.
[32] K. Drouiche, "A new test for whiteness," *IEEE Trans. Signal Process.*, vol. 48, no. 7, pp. 1864–1871, Jul. 2000.

Jie Cui (S'99) completed undergraduate studies in automatic control from Nanjing Institute of Mechanical Technology (NIMT), China, in 1992. He received the M.E. degree in biomedical engineering from the Southeast University (Medical Electronics Lab), Nanjing, Jiangsu Province, China, in 1998 and M.S. degree in biomedical science from the University of Saskatchewan (Medical Imaging Lab), Saskatoon, SK, Canada, in 2001. Since September 2001, he has been working towards the Ph.D. degree in the Institute of Biomaterials and Biomedical Engineering (Sensory Communication Lab), University of Toronto.

From 1993 to 1995, he was a Research and Design Engineer at the Department of Automatic Control at NIMT. His research interests include pattern recognition, time-frequency analysis of biomedical signals, wavelets, chirplets, as well as vision science and technology.

Willy Wong (M'00) received his first formal education in music. Later he received the B.Sc. degree in physics and the Ph.D. degree in physics and biomedical engineering from the University of Toronto, Toronto, ON, Canada, in 1992 and 1996, respectively.

He has held visiting positions in Japan, the U.K., and the Netherlands. Currently he is Assistant Professor at the Edward S. Rogers, Sr. Department of Electrical and Computer Engineering with a cross-appointment at the Institute of Biomaterials and Biomedical Engineering (IBBME) and the Collaborative Program in Neuroscience. He is also option chair (biomedical) for the Division of Engineering Science at the University of Toronto. His research interests are in biological sensory systems with an emphasis on signal processing, algorithm design, modelling, and psychology.